

This article was downloaded by:

On: 25 January 2011

Access details: *Access Details: Free Access*

Publisher *Taylor & Francis*

Informa Ltd Registered in England and Wales Registered Number: 1072954 Registered office: Mortimer House, 37-41 Mortimer Street, London W1T 3JH, UK



Separation Science and Technology

Publication details, including instructions for authors and subscription information:

<http://www.informaworld.com/smpp/title~content=t713708471>

Study of Nonlinear Wave Propagation Theory. III. Removing Heavy Metals from Wastewater by Ion-Exchange Process

Jia -Ming Chern^a; Fang -Ching Chang^a

^a DEPARTMENT OF CHEMICAL ENGINEERING, TATUNG UNIVERSITY, TAIPEI, TAIWAN, REPUBLIC OF CHINA

Online publication date: 19 June 2000

To cite this Article Chern, Jia -Ming and Chang, Fang -Ching(2000) 'Study of Nonlinear Wave Propagation Theory. III. Removing Heavy Metals from Wastewater by Ion-Exchange Process', *Separation Science and Technology*, 35: 8, 1099 – 1116

To link to this Article: DOI: 10.1081/SS-100100214

URL: <http://dx.doi.org/10.1081/SS-100100214>

PLEASE SCROLL DOWN FOR ARTICLE

Full terms and conditions of use: <http://www.informaworld.com/terms-and-conditions-of-access.pdf>

This article may be used for research, teaching and private study purposes. Any substantial or systematic reproduction, re-distribution, re-selling, loan or sub-licensing, systematic supply or distribution in any form to anyone is expressly forbidden.

The publisher does not give any warranty express or implied or make any representation that the contents will be complete or accurate or up to date. The accuracy of any instructions, formulae and drug doses should be independently verified with primary sources. The publisher shall not be liable for any loss, actions, claims, proceedings, demand or costs or damages whatsoever or howsoever caused arising directly or indirectly in connection with or arising out of the use of this material.

Study of Nonlinear Wave Propagation Theory. III. Removing Heavy Metals from Wastewater by Ion-Exchange Process

JIA-MING CHERN* and FANG-CHING CHANG

DEPARTMENT OF CHEMICAL ENGINEERING

TATUNG UNIVERSITY

40 CHUNGSHAN NORTH ROAD, 3RD SEC., TAIPEI 104, TAIWAN, REPUBLIC OF CHINA

ABSTRACT

The nonlinear wave propagation theory has been applied to predict the breakthrough and regeneration curves of ion-exchange columns for heavy metal removal. Batch experimental tests using IRC-718 cationic resin were conducted to obtain the ion-exchange equilibria of H/Cu and H/Ni systems, and column tests were conducted to obtain the breakthrough and regeneration curves under various operating conditions. The batch experimental results show that the affinity sequence is Cu > H > Ni. The column experimental results show that IRC-718 in H-form is effective for removing copper from synthetic wastewater but not effective for nickel removal. For a copper-rich feed solution, the ion-exchange wave is a self-sharpening wave and its regeneration wave is a nonsharpening one. For a nickel-rich feed solution, the ion-exchange wave is a nonsharpening wave and its regeneration wave is a self-sharpening one. For a copper/nickel mixture feed, nickel gradually appears in the effluent, and a plateau of concentration higher than the feed one is identified. Simple equations based on the nonlinear wave propagation theory have been developed to predict the breakthrough and regeneration curves, and the predicted results are quite comparable with the experimental data.

Key Words. Ion exchange; Dynamics; Wave propagation; Heavy metal; Wastewater

* To whom correspondence should be addressed. Telephone: 011886225925252 ext. 3487. FAX: 011886225861939. E-mail: JMCHERN@CHE.TTIT.EDU.TW

INTRODUCTION

Due to limited water resources and increasing water demands of various kinds, especially of industries, how to treat and reuse industrial wastewater has become not only a very important problem to environmental protection but also a crucial issue to industries seeking sustainable development. Wastewater containing heavy metals is one of the most difficult industrial wastewater to treat. The common methods to treat heavy metal-containing wastewater include chemical precipitation, ion exchange, activated alumina, reverse osmosis, and electrodialysis. Although the conventional chemical precipitation method, which is the most popular method used in Taiwan, is quite effective in removing heavy metals from wastewater, the resulting large quantity of heavy metal-containing sludge is very tough to deal with and has caused secondary pollution problems. On the contrary, ion-exchange processes are also very efficient but generate much less sludge. Moreover, different heavy metals can be separated and recovered, and the ideal state of so-called zero discharge can be approached via adequate ion exchange-resin selection, process design, column operation, and in combination with other posttreatments. Therefore, the ion-exchange process is one of the most promising treatment technologies for heavy metal-containing wastewater.

The methodology for ion-exchange process design is quite straightforward and has been well documented (1, 2). Most research on ion exchange can be broadly classified into two categories: resin/ion properties studies and treatability studies. The former emphasizes the ion exchanger resin and exchanged ion interaction, including equilibrium relationship, effect of ion concentration, pH, complexion agents, ionic strength, and resin modification (3–6). The latter emphasizes the treatability of different ion-exchange resins for different cations or anions, including effluent cation or anion concentrations, stability of resin after cyclic operations, and regeneration capacity (7–9). Except for a few works done by Clifford and his coworkers (10–13), the dynamic behavior of ion-exchange columns used in wastewater treatment processes has received relatively little attention. In operational practice an ion-exchange cycle is carried out until the effluent metal concentrations, which can be indicated by density or conductivity measurement, are greater than acceptable levels. Then backwash, regeneration, and rinse cycles are carried out to restore the ion exchanger capacity for the next ion-exchange cycle. From the standpoint of heavy metal removal only, this approach is simple and has been widely used in water and wastewater treatment practice. However, if heavy metal separation and recovery are desired, we need to know what kind of heavy metal will exit an ion-exchange column at what time period. Then we can collect the effluent solutions and separate different heavy metals. In order to know what kind of metal ion exits an ion-exchange column at what time period, we need to know the dynamic behavior of the column.



The dynamic behavior of ion-exchange columns is governed by a set of differential equations coupled with a set of algebraic equations. One can either solve that set of differential equations to obtain the column dynamics or use the concept of wave propagation to depict the column dynamics without actually solving the differential equations. We therefore initiated a series of studies aimed at applying the nonlinear wave propagation theory to predict the column dynamic behaviors of fixed-bed operations in pollution control applications. The first two parts of this series demonstrated that the nonlinear wave propagation theory indeed gives satisfactory predictions of the column dynamics of dye/carbon systems (14, 15). This paper continues to present the results of our experimental and theoretical investigation of heavy metal ion-exchange processes.

THEORETICAL BASIS

The theoretical basis of this study is directly built upon the nonlinear wave propagation theory (16–21). The wave that was previously called “boundary,” “transition,” “front,” or “mass transfer zone” is defined as a moving concentration variation. The column dynamics of such system in a fixed bed can be described by the following governing equation:

$$(1 - \varepsilon) \frac{\partial \bar{C}_i}{\partial t} + \varepsilon \frac{\partial C_i}{\partial t} + u_0 \varepsilon \frac{\partial C_i}{\partial Z} = 0, \quad i = 1, 2, \dots, n \quad (1)$$

where C_i is the concentration of exchangeable ion i in the mobile phase, \bar{C}_i is the concentration of exchangeable ion i in the stationary phase, ε is the void fraction of the bed, u_0 is the linear velocity of the carrier fluid, t is the operating time, and Z is the distance from the inlet of the mobile phase. The assumptions associated with Eq. (1) are:

- Local ion exchange equilibria: $\bar{C}_i = f_i(C_1, C_2, \dots, C_n)$
- No other chemical reactions involved
- Exclusion of co-ions and nonionic species from the resin interior
- Constant binary separation factors
- No shrinking or swelling of resin
- Ideal plug flow
- Mass transfer in flow direction by convection only
- Isothermal behavior
- Unity activity coefficients

With proper initial and boundary conditions specified, which depend upon operating conditions, Eq. (1) can be solved for C_i as a function of Z and t . The breakthrough curve, which is often experimentally determined, is the effluent history, $C_i(Z = L, t)$. In general, the ion-exchange equilibria are highly cou-



pled, i.e., there exist complicated interactions among the exchangeable ions. One can expect that solving the governing equations is rather tedious, even using a fast personal computer and a proper numerical technique such as the finite difference method.

Instead of directly solving the governing equations, Helfferich and his coworkers (12–18) used the concept of wave velocity defined as

$$u_{C_i} \equiv \left(\frac{\partial Z}{\partial t} \right)_{C_i}, \quad i = 1, 2, \dots, n \quad (2)$$

to describe the column dynamics. This is the velocity at which a given constant concentration C_i travels through the ion-exchange column. Combining Eqs. (1) and (2) leads to

$$u_{C_i} = \frac{u_0}{1 + \frac{1-\varepsilon}{\varepsilon} \left(\frac{\partial \bar{C}_i}{\partial C_i} \right)_Z}, \quad i = 1, 2, \dots, n \quad (3)$$

Equation (3) is used to calculate the concentration wave velocity of nonsharpening waves. For self-sharpening waves, the concentration wave velocity is calculated by the following equation:

$$u_{\Delta C_i} = \frac{u_0}{1 + \frac{1-\varepsilon}{\varepsilon} \left(\frac{\Delta \bar{C}_i}{\Delta C_i} \right)_Z}, \quad i = 1, 2, \dots, n \quad (4)$$

Once the concentration wave velocity is known, the column dynamics can be easily predicted.

H⁺/M²⁺ ION-EXCHANGE SYSTEMS

The above nonlinear wave propagation theory can be used to predict the column dynamics of binary ion-exchange systems. Consider a binary system with only two exchangeable cations, H⁺ and M²⁺. The concentration wave velocity can be converted to

$$u_{X_M} = \frac{u_0}{1 + \left(\frac{1-\varepsilon}{\varepsilon} \right) \left(\frac{\bar{C}}{C} \right) \left(\frac{dY_M}{dX_M} \right)_Z} \quad (5)$$

where X_M and Y_M are the equivalence fractions of M²⁺ in the mobile phase and the stationary phase, respectively; C and \bar{C} are the total mobile phase concentration and the ion exchanger capacity, respectively.

For the H⁺/M²⁺ binary system, the equilibrium relationship of the two exchangeable ions can be represented by the so-called separation factor, which



is defined as

$$\alpha_{\text{MH}} = \frac{Y_{\text{MH}} X_{\text{H}}}{X_{\text{M}} Y_{\text{H}}} \quad (6)$$

Since the summations of the two equivalence fractions are both equal to unity, one can express Y_{M} in terms of X_{M} by using the definition of the separation factor:

$$Y_{\text{M}} = \frac{\alpha_{\text{MH}} X_{\text{M}}}{1 - X_{\text{M}} + \alpha_{\text{MH}} X_{\text{M}}} \quad (7)$$

The partial derivative in the denominator of Eq. (5) therefore becomes

$$\frac{dY_{\text{M}}}{dX_{\text{M}}} = \frac{\alpha_{\text{MH}}}{(1 - X_{\text{M}} + \alpha_{\text{MH}} X_{\text{M}})^2} \quad (8)$$

If the affinity of the heavy metal ion to the cation resin is greater than that of the hydrogen ion, then α_{MH} is greater than unity. In this case a feed of heavy metal-containing solution to a resin bed presaturated with hydrogen ion will result in a self-sharpening wave of the heavy metal concentration variation. The cumulative effluent volume at breakthrough is calculated by the following equation:

$$V = \varepsilon V_b \left[1 + \left(\frac{1 - \varepsilon}{\varepsilon} \right) \left(\frac{\bar{C}}{C} \right) \frac{Y_{\text{MF}} - Y_{\text{MP}}}{X_{\text{MF}} - X_{\text{MP}}} \right] \quad (9)$$

where V_b is the bed volume and the subscripts F and P represent the feed and presaturation conditions, respectively. Combining Eqs. (7) and (9) leads to

$$V = \varepsilon V_b \left[1 + \left(\frac{1 - \varepsilon}{\varepsilon} \right) \left(\frac{\bar{C}}{C} \right) \frac{\alpha_{\text{MH}}}{(1 - X_{\text{MF}} + \alpha_{\text{MH}} X_{\text{MF}})(1 - X_{\text{MP}} + \alpha_{\text{MH}} X_{\text{MP}})} \right] \quad (10)$$

The regeneration wave for the above self-sharpening ion-exchange wave is a nonsharpening one, and the cumulative effluent volume for a given effluent concentration is calculated by the following equation:

$$V = \varepsilon V_b \left[1 + \left(\frac{1 - \varepsilon}{\varepsilon} \right) \left(\frac{\bar{C}}{C} \right) \frac{\alpha_{\text{MH}}}{(1 - X_{\text{M}} + \alpha_{\text{MH}} X_{\text{M}})^2} \right] \quad (11)$$

It is important to note that the total mobile phase concentration in Eq. (11) is usually much greater than that in Eq. (10) because concentrated acid solution is usually used to regenerate the ion-exchange bed.

If the affinity of the heavy metal ion to the cation resin is lower than that of the hydrogen ion, then α_{MH} is less than unity. In this case a feed of heavy



metal-containing solution to a resin bed presaturated with hydrogen ion will result in a nonsharpening wave of the heavy metal concentration variation. The cumulative effluent volume for a given effluent concentration is calculated by Eq. (11). The regeneration wave for the nonsharpening ion-exchange wave is a self-sharpening one, and the cumulative effluent volume for a given effluent concentration is calculated by Eq. (10).

H⁺/M₁²⁺/M₂²⁺ ION-EXCHANGE SYSTEMS

Consider a tertiary ion-exchange system with affinity sequence 1 > 2 > 3 and the binary separation factors defined as

$$\alpha_{12} = \frac{Y_1 X_2}{X_1 Y_2} \quad \text{and} \quad \alpha_{13} = \frac{Y_1 X_3}{X_1 Y_3} \quad (12)$$

Since the summation of the three equivalence fractions is equal to unity, by using the definition of the separation factors, one can express Y_i in terms of X_i :

$$Y_1 = \frac{\alpha_{12}\alpha_{13}X_1}{\alpha_{12}\alpha_{13}X_1 + \alpha_{13}X_2 + \alpha_{12}(1 - X_1 - X_2)} = f_1(X_1, X_2) \quad (13)$$

$$Y_2 = \frac{\alpha_{13}X_2}{\alpha_{12}\alpha_{13}X_1 + \alpha_{13}X_2 + \alpha_{12}(1 - X_1 - X_2)} = f_2(X_1, X_2) \quad (14)$$

The coherence condition for this system is

$$\frac{dY_1}{dX_1} = \frac{dY_2}{dX_2} = \lambda \quad (15)$$

This coherence condition results in an eigenvalue problem

$$\begin{bmatrix} \frac{\partial f_1}{\partial X_1} - \lambda & \frac{\partial f_1}{\partial X_2} \\ \frac{\partial f_2}{\partial X_1} & \frac{\partial f_2}{\partial X_2} - \lambda \end{bmatrix} \begin{bmatrix} dX_1 \\ dX_2 \end{bmatrix} = \begin{bmatrix} 0 \\ 0 \end{bmatrix} \quad (16)$$

The two eigenvalues can be solved from the following quadratic equation:

$$\lambda^2 - \left(\frac{\partial f_1}{\partial X_1} + \frac{\partial f_2}{\partial X_2} \right) \lambda + \frac{\partial f_1}{\partial X_1} \frac{\partial f_2}{\partial X_2} - \frac{\partial f_1}{\partial X_2} \frac{\partial f_2}{\partial X_1} = 0 \quad (17)$$

Once the eigenvalues are obtained, the concentration wave velocities can be calculated as follows:

$$u_{\text{slow}} = \frac{u_0}{1 + \frac{1 - \varepsilon}{\varepsilon} \frac{\bar{C}}{C} \lambda_{\text{large}}} \quad (18)$$



$$u_{\text{fast}} = \frac{u_0}{1 + \frac{1-\varepsilon}{\varepsilon} \frac{\bar{C}}{C} \lambda_{\text{small}}} \quad (19)$$

Of the two eigenvalues, the larger one corresponds to the slow wave while the smaller one corresponds to the fast wave. When the two eigenvalues are equal, the watershed point in the composition path diagram can be located:

$$\begin{cases} X_1 = \frac{\alpha_{12} - 1}{\alpha_{13} - 1} \\ X_2 = 0 \end{cases} \quad (20)$$

The composition path diagram can then be easily constructed. All paths which are straight lines can be plotted with the help of a rule of equal intercept ratio (18). The composition route is the pathway for which the concentration waves meet the coherence condition. If the wave velocity in the upward moving stream is faster than that in the downward moving stream, the wave is self-sharpening, and the concentration wave velocity, as shown in Eqs. (18) and (19), should be modified as

$$u_{\text{slow}} = \frac{u_0}{1 + \frac{1-\varepsilon}{\varepsilon} \frac{\bar{C}}{C} \Lambda_{\text{large}}} \quad (21)$$

$$u_{\text{fast}} = \frac{u_0}{1 + \frac{1-\varepsilon}{\varepsilon} \frac{\bar{C}}{C} \Lambda_{\text{small}}} \quad (22)$$

where Λ_{large} and Λ_{small} are the two eigenvalues satisfying the following integral coherence condition:

$$\frac{\Delta Y_1}{\Delta X_1} = \frac{\Delta Y_2}{\Delta X_2} = \Lambda \quad (23)$$

With the composition path diagram, the breakthrough curve for individual ions can be easily predicted. The column effluent contains three composition zones: the presaturation composition comes out first, followed by the intermediate composition and the feed composition.

EXPERIMENTAL

Amberlite IRC-718 (Rohm and Haas, USA) was used as the cationic-exchange resin in this study. It was repeatedly conditioned with analytical grade HCl and NaOH (Yakuri, Japan) before use. The capacity of the resin in hydrogen form was determined by the column method, and the binary separation



factors for the $\text{Cu}^{2+}/\text{H}^+$ and $\text{Ni}^{2+}/\text{H}^+$ systems were determined by batch tests (22). In the batch tests, different amounts of the resin were put in several plastic bottles, each filled with 100 mL of cupric nitrate or nickel nitrate (Katayama, Japan) solution. All the bottles were placed in a temperature-controlled shaker (Hotech, Model 706) and shaken for 24 hours to reach equilibrium. The solution pH and metal concentrations were measured by a pH meter (AION, model PHB-9901) and an atomic absorption spectrophotometer (Varian, model 3000), respectively. The equilibrium metal equivalence fraction in the resin phase versus that in the solution phase was plotted, and the formula developed by Clifford (10) was used to calculate the average binary separation factors.

In the ion-exchange column tests, synthetic wastewater was fed to the top of a glass column of 15 mm I.D. and 600 mm long filled with resin in hydrogen form. The bed void fraction was measured to be 0.4. The flow rate was controlled by a metering pump (Watson-Marlow, model 302S) to be 2 bed volumes (BV) per hour. The effluent samples were collected at varying times by a fraction collector (ISCO, model Retriever 500); the sample pH and the

TABLE 1
Experimental Conditions for Ion-Exchange Column Tests

Run	Presaturation	Feed	Remark
1	Resin in H-form	$C_{\text{Cu}} = 120 \text{ ppm}$, pH 5.47	First copper exchange cycle
2	$C_{\text{Cu}} = 120 \text{ ppm}$, pH 5.47	2.5 M H_2SO_4	First copper regeneration cycle
3	$C_{\text{Cu}} = 0.01 \text{ ppm}$, very low pH	$C_{\text{Cu}} = 176 \text{ ppm}$, pH 5.43	Second copper exchange cycle
4	$C_{\text{Cu}} = 176 \text{ ppm}$, pH 5.43	0.25 M H_2SO_4	Second copper regeneration cycle
5	Resin in H-form	$C_{\text{Ni}} = 87 \text{ ppm}$, pH 6.86	First nickel exchange cycle
6	$C_{\text{Ni}} = 87 \text{ ppm}$, pH 6.86	0.1 M H_2SO_4	First nickel regeneration cycle
7	$C_{\text{Ni}} = 0.01 \text{ ppm}$, very low pH	$C_{\text{Ni}} = 333 \text{ ppm}$, pH 6.80	Second nickel exchange cycle
8	$C_{\text{Ni}} = 333 \text{ ppm}$, pH 6.80	0.1 M H_2SO_4	First nickel regeneration cycle
9	Resin in H-form	$C_{\text{Cu}} = 159 \text{ ppm}$, $C_{\text{Ni}} = 164 \text{ ppm}$, pH 5.71	First copper/nickel exchange cycle
10	$C_{\text{Cu}} = 159 \text{ ppm}$, $C_{\text{Ni}} = 164 \text{ ppm}$, pH 5.71	0.1 M H_2SO_4	First copper/nickel regeneration cycle



metal concentrations were measured. In the regeneration column tests, diluted sulfuric acid was fed to the column and the effluent samples were collected for pH and metal analysis. All the column experiments were carried out in an air-conditioned room with a temperature of $25 \pm 1^\circ\text{C}$. The experimental conditions for the column test runs are summarized in Table 1.

RESULTS AND DISCUSSION

Since the ion exchanger resin used in this study has weak acid groups, its capacity is not constant during the ion-exchange process. The capacity should increase with increasing solution pH. Moreover, the apparent selectivity for heavy metal also depends upon the solution pH according to the technical data sheet provided by Rohm and Haas. The ion-exchange equilibria between heavy metal ions and hydrogen ion should be more appropriately represented by the selectivity coefficient instead of a constant separation factor because heavy metal ions are divalent and hydrogen ion is monovalent. In order to use the conventional wave theory for prediction, however, we neglect the variation of the resin capacity and use a constant separation factor to represent the ion-exchange equilibrium in this paper. The prediction of column dynamics using selectivity coefficients and taking account of any complexion between heavy metal ion and hydroxide ion will be presented in a separate paper.

The resin capacity in the hydrogen form was measured to be 1.87 meq/mL wet resin, and the average binary separation factors for the $\text{Cu}^{2+}/\text{H}^+$ and $\text{Ni}^{2+}/\text{H}^+$ systems were $\alpha_{\text{CuH}} = 2.42$ and $\alpha_{\text{NiH}} = 0.28$, respectively. In general, as a metal-rich solution is fed to a column presaturated with hydrogen ion, the metal ion will exchange with the hydrogen ion in the resin. The effluent metal concentration remains at a very low level and then increases sharply or gradually to the feed concentration, depending upon the nature of the concentration wave. For a cumulative effluent volume of less than 0.4 BV, the effluent pH initially equals the in-pore solution pH and then increases sharply or gradually. Figure 1 shows a typical effluent metal concentration and pH of a column test run.

Since the affinity of copper to the resin is stronger than that of hydrogen ion ($\alpha_{\text{CuH}} > 1$), the ion-exchange wave resulting from a feed of copper-rich solution to a hydrogen-presaturated bed is a self-sharpening one. Ideally, this self-sharpening wave will develop into a shock; the feed composition travels along the column and pushes the presaturation composition downward with a sharp boundary. The breakthrough volume for the self-sharpening wave is calculated by Eq. (10).

Figure 2 shows the experimental and predicted breakthrough curves for two column test runs with feed copper concentrations of 120 and 176 ppm, respectively. In Fig. 2 the empty and filled circles represent the experimental



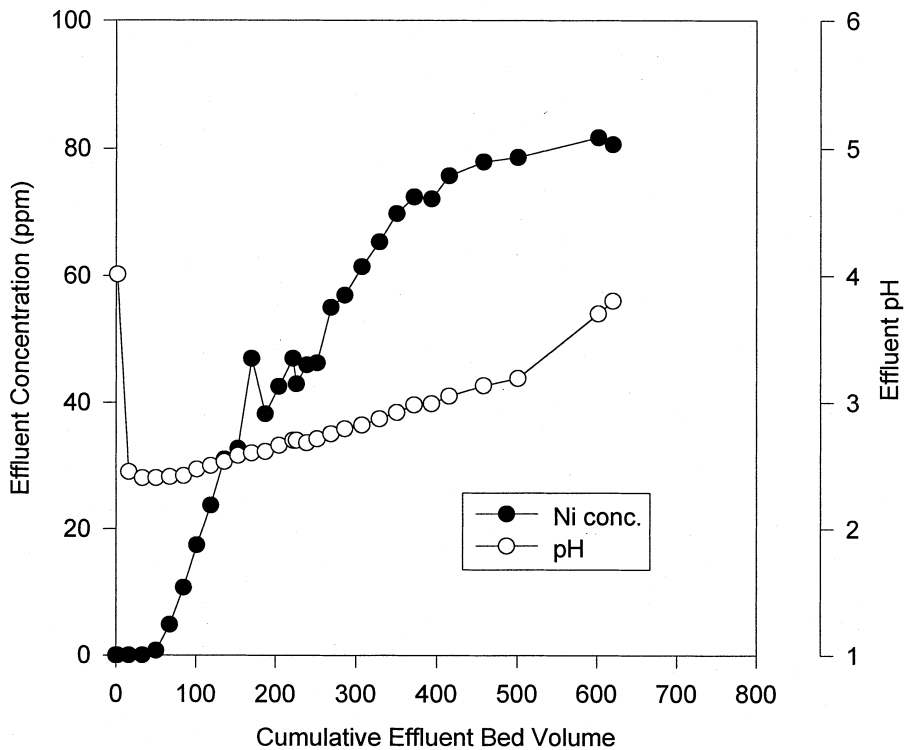


FIG. 1 A typical effluent metal concentration and pH versus cumulative effluent bed volume.

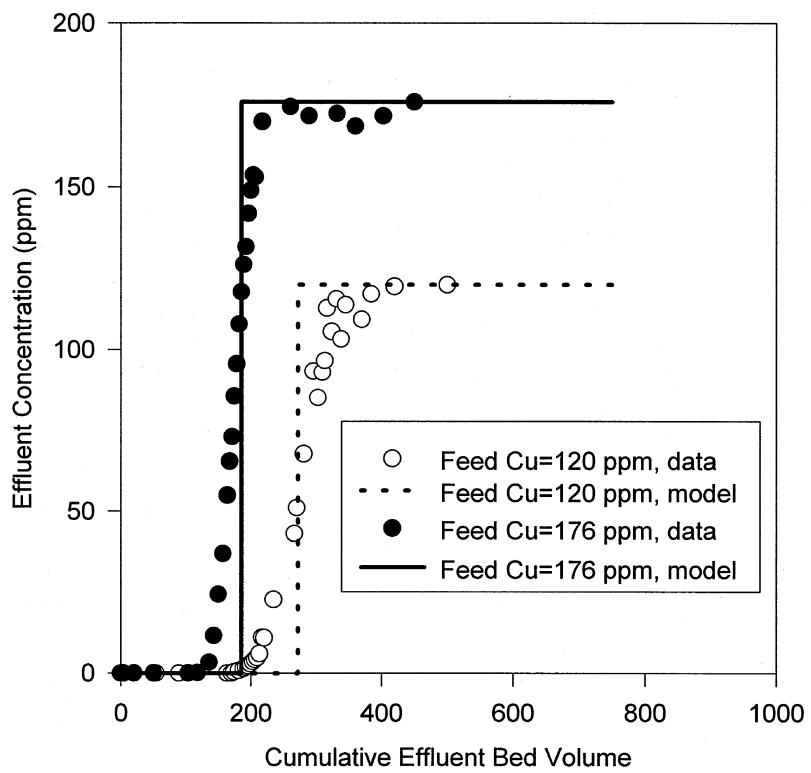


FIG. 2 The comparison of predicted and experimental breakthrough curves of two column test runs with different feed copper concentrations.

data while the solid and dashed lines represent the predicted breakthrough curves. For these two column tests, the presaturated copper equivalence fractions are both zero and the feed copper equivalence fractions are very close to unity. Therefore, the breakthrough volume decreases with increasing feed concentration according to Eq. (10). The nonlinear wave propagation theory predicts that feed concentrations of 120 and 176 ppm will breakthrough at 272 and 185 bed volumes, respectively. The experimental data show, however, that the effluent copper concentration is greater than 3 ppm, the discharge standard in Taiwan, because the cumulative effluent volume is greater than 202 BV for the 120 ppm feed and 135 BV for the 176 ppm feed, respectively. Obviously, ion-exchange processes are more effective for diluted heavy metal solutions because the heavy metal is more preferred by the resin in diluted solutions and larger amounts of wastewater can be treated in the same column. In fact, selectivity reversal occurs for high feed copper concentrations, and this phenomenon will be discussed in a separate paper.

It is important to note that the resin capacity and the separation factor used in the calculations were determined from independent batch experiments; they were not treated as adjustable parameters to best fit the breakthrough curves. One can see from Fig. 2 that the calculated results are quite comparable with the experimental data. However, due to the finite mass-transfer rate and the axial dispersion effect, the experimental breakthrough curves look like S shapes instead of sharp steps. To model the S-shaped breakthrough curves, one needs a more sophisticated model with parameters such as the axial dispersion coefficient and the ion-exchange rate constant that are usually difficult to determine independently. The nonwave propagation theory therefore serves as a simple tool to predict the breakthrough curves of ion-exchange column operations, and its predicted results are still satisfactory.

After the ion-exchange bed was saturated with the copper-rich solution, it was regenerated by sulfuric acid. The resulting regeneration wave became a non-sharpening one, and the cumulative effluent volume was calculated by Eq. (11). Figure 3 shows a comparison of the experimental and predicted regeneration curves for a typical regeneration test run. In this test run the column was presaturated with 176 ppm copper solution and regenerated by 0.25 M sulfuric acid. At the beginning of regeneration, the feed sulfuric acid pushed out the liquid previously in the bed. Therefore, the effluent copper concentration is theoretically equal to 176 ppm for $V = 0$ to 0.4 BV. After 0.4 BV, the ion-exchange resin starts to contact the feed sulfuric acid and releases copper to the mobile phase. Since the total mobile-phase concentration during regeneration is very high, the resulting effluent copper concentration immediately jumps to 8238 ppm, the mobile-phase concentration in equilibrium with 0.25 M sulfuric acid. The effluent copper concentration remains at 8238 ppm from $V = 0.4$ BV to $V = 2.2$ BV, then gradually decreases to zero after



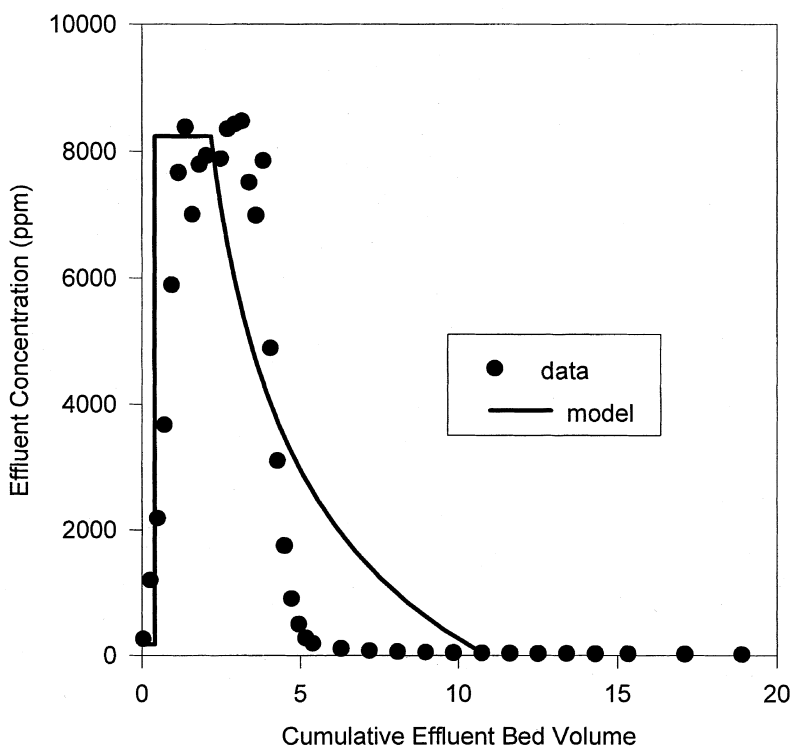


FIG. 3 The comparison of predicted and experimental regeneration curves of a column presaturated with 176 ppm copper solution and regenerated by 0.25 M sulfuric acid.

$V > 2.2$ BV. As shown in Fig. 3, the predicted regeneration curve is also comparable with the experimental data. The model predicts that the effluent copper concentration becomes zero at $V = 10.9$ BV. However, the experimental effluent copper concentration approaches zero earlier than 10.9 BV. Judging from the experimental regeneration curve, the regeneration wave looks like a self-sharpening one, not a nonsharpening one. But according to the results of our batch equilibrium study, for $\alpha_{\text{CuH}} > 1$ the regeneration wave is a non-sharpening one. This discrepancy suggests that the representation of the ion-exchange equilibrium by a constant separation factor at high ionic strength is probably inadequate. The ionic strength is much higher in the regeneration cycle than in the exchange cycle, and therefore selectivity reversal may occur, i.e., the separation factor α_{CuH} at high ionic strength should be less than unity. Obviously, more suitable ion-exchange equilibrium models need to be developed.

Since the affinity of nickel to the resin is weaker than that of hydrogen ion ($\alpha_{\text{NiH}} < 1$), the ion-exchange wave resulting from a feed of nickel-rich solution to a hydrogen-presaturated bed is a nonsharpening one. Ideally, this nonsharpening wave will develop into a proportionate pattern with the breakthrough volume calculated by Eq. (11). Figure 4 shows the experimental and predicted breakthrough curves for two column test runs with feed nickel con-



centrations of 87 and 333 ppm, respectively. Again, the nonlinear wave propagation theory predicts that the higher feed concentration breakthroughs earlier than the lower ones. Obviously, nickel ion cannot be effectively removed by the resin in H-form because the effluent nickel concentration breakthroughs occur very soon.

The regeneration wave for a nonsharpening ion-exchange wave is a self-sharpening one. Figure 5 shows the experimental and predicted regeneration curves for a column presaturated with 87 ppm nickel solution and regenerated by 0.1 M sulfuric acid. At the beginning of regeneration the effluent nickel concentration is theoretically equal to 87 ppm for $V = 0$ to 0.4 BV. At $V = 0.4$ BV the effluent nickel concentration jumps to 3194 ppm and remains at that concentration up to $V = 10.7$ BV. At $V = 10.7$ BV the effluent nickel concentration drops to zero, according to the theory. Again, the discrepancy between the predicted and experimental regeneration curves may result from the axial dispersion effect and finite the ion-exchange rate that are neglected by the theory.

For the Cu/Ni/H tertiary ion-exchange system, the affinity sequence is Cu > H > Ni. The separation factors are $\alpha_{12} = 2.42$ and $\alpha_{13} = 2.42/0.28 = 8.64$. The watershed points for this system are $X_2 = 0$ and $X_1 = (2.42 - 1)/(8.64 -$

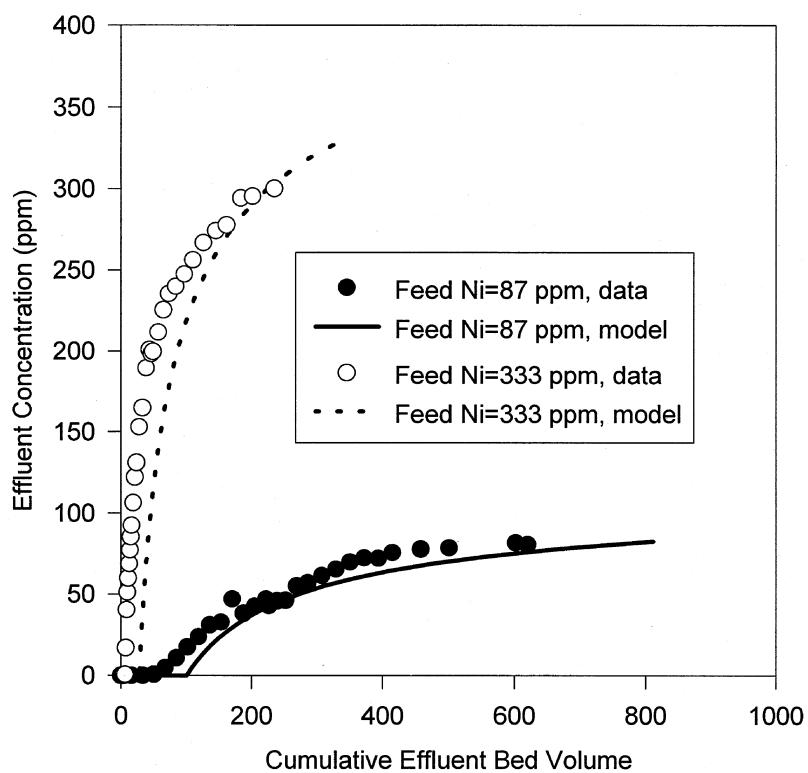


FIG. 4 The comparison of predicted and experimental breakthrough curves of two column test runs with different feed nickel concentrations.



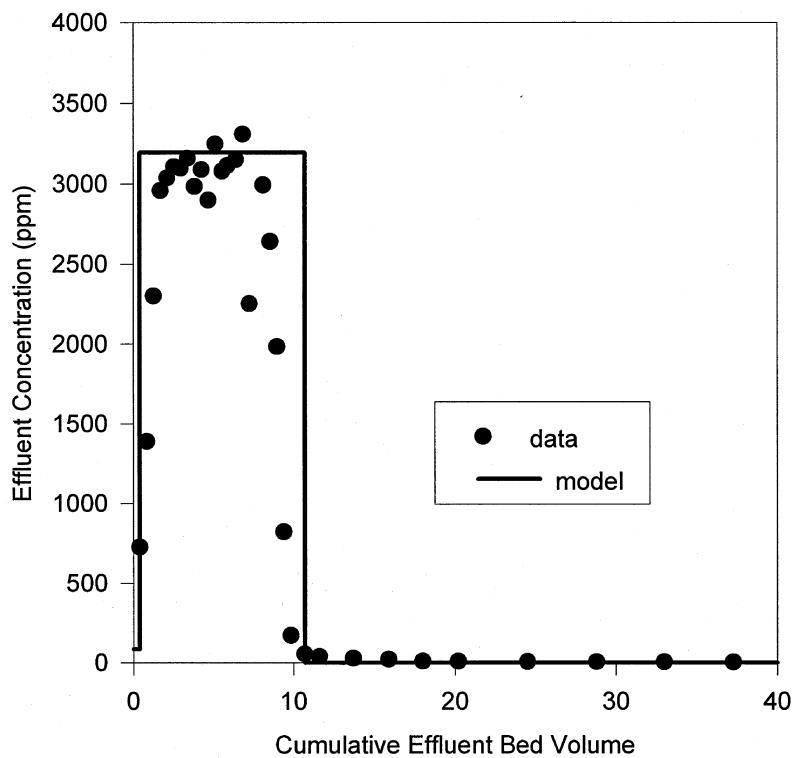


FIG. 5 The comparison of predicted and experimental regeneration curves of a column presaturated with 87 ppm nickel solution and regenerated by 0.1 M sulfuric acid.

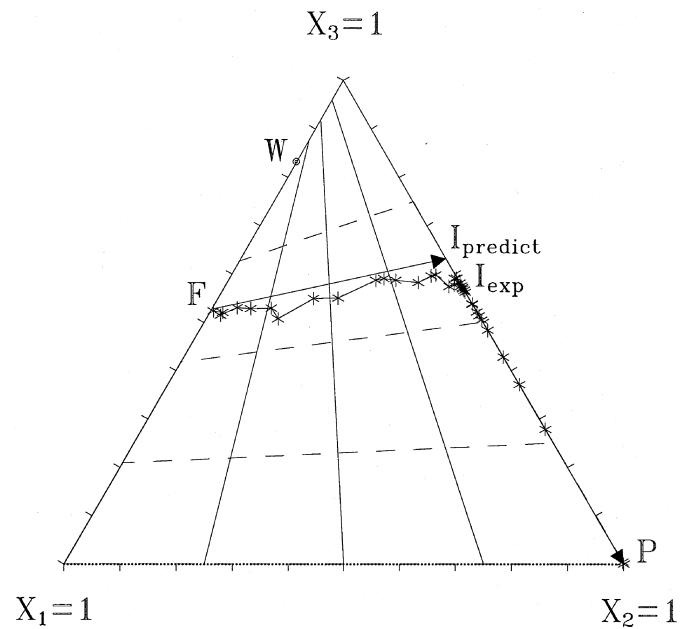


FIG. 6 The predicted and experimental composition routes for Cu/Ni/H system-exchange cycle.



1) = 0.19. The composition path diagram constructed is shown in Fig. 6 where dashed lines represent the slow paths and solid lines the fast paths, F is the feed composition, P is the presaturation composition, I is the intermediate composition, and W is the watershed point. Also shown in Fig. 6 are the predicted and experimental composition routes of the ion-exchange cycle. The predicted composition route starts from the feed composition point, takes the slow path, then switches to the fast path that leads to the presaturation composition point. In Fig. 6 the eigenvalues decrease along the slow composition route ($F \rightarrow I$); the resulting concentration wave is a self-sharpening one and the wave velocity is calculated by Eq. (21). The eigenvalues increase along the fast composition route ($I \rightarrow P$); the resulting concentration wave is a nonsharpening one and the wave velocity is calculated by Eq. (19). With the composition path diagram and the composition route established, we can calculate the breakthrough curves for copper and nickel, and the results are shown in Fig. 7.

As is seen from Fig. 7, the nonlinear wave propagation theory using a constant resin capacity and constant separation factors can predict the break-

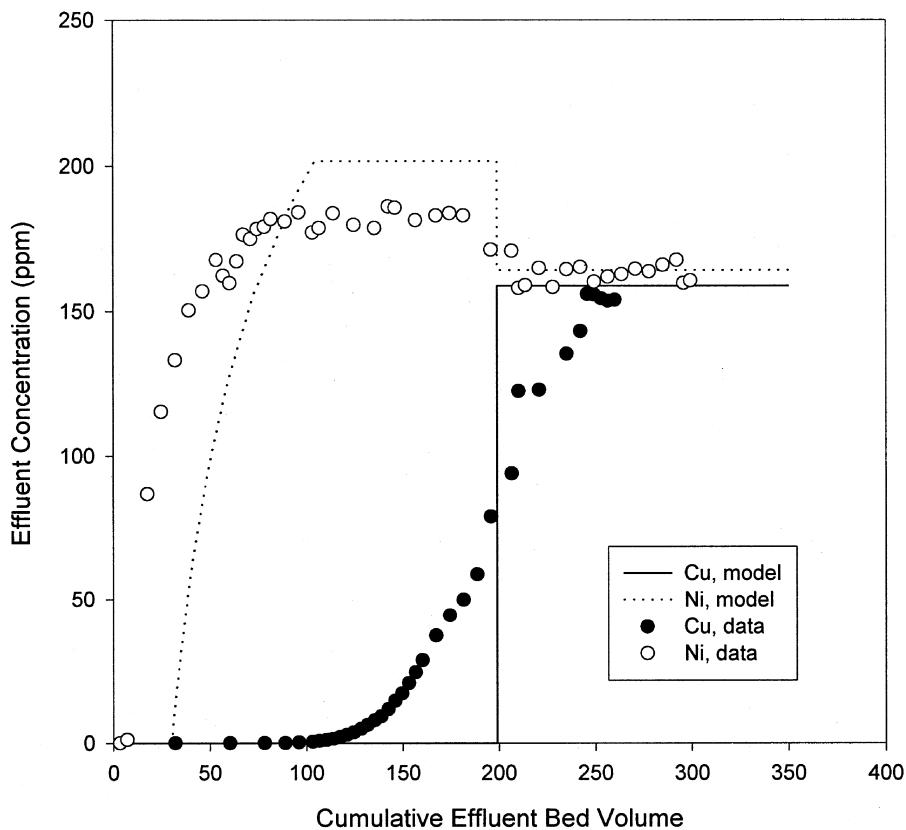


FIG. 7 The comparison of predicted and experimental breakthrough curves of Cu/Ni/H system.



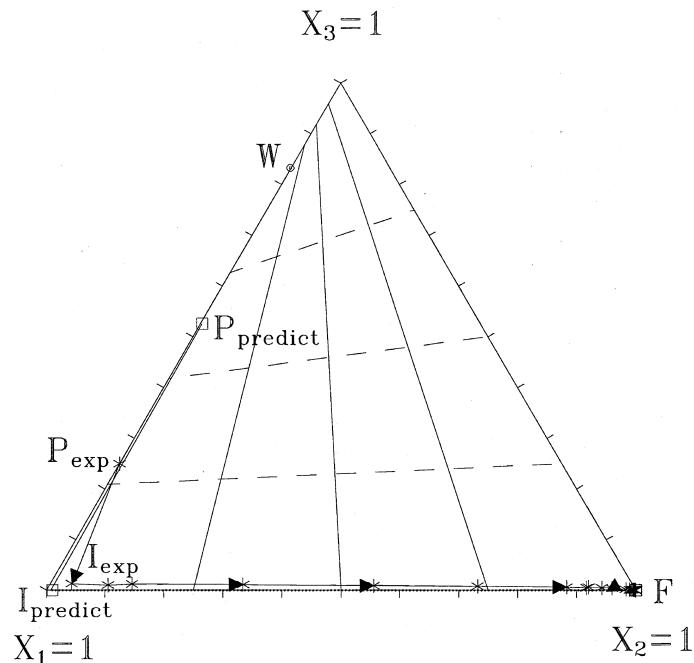


FIG. 8 The predicted and experimental composition routes for Cu/Ni/H system-regeneration cycle.

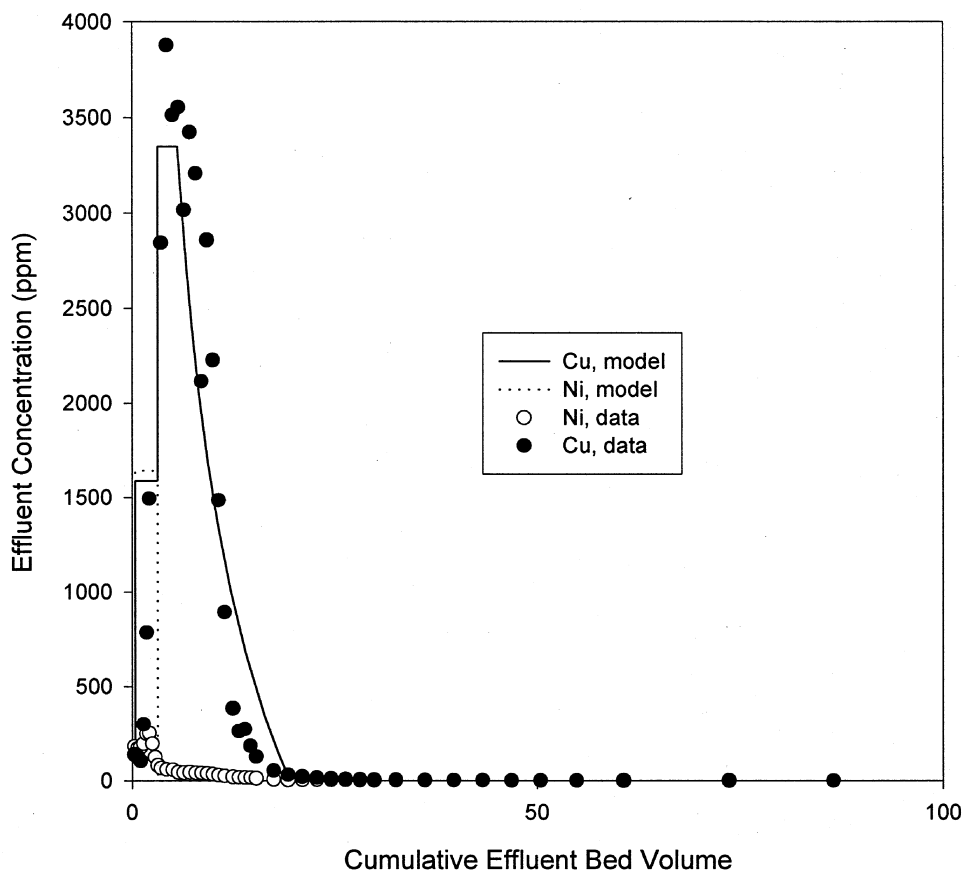


FIG. 9 The comparison of predicted and experimental regeneration curves of Cu/Ni/H system.

through curves only qualitatively. To get a better prediction, we will attempt to develop a more sophisticated model will be in the future.

The composition path diagram and the regeneration curves of the regeneration cycle can also be obtained, as shown in Figs. 8 and 9, respectively.

According to the experimental and theoretical results, the proposed operating strategy for copper and nickel separation is as follows:

- Collect the effluent before 100 bed volumes to get a nickel-rich solution in the exchange cycle.
- Collect the effluent between 3 and 20 bed volumes to get a copper-rich solution in the regeneration cycle.

CONCLUSIONS

The chelating resin IRC-718 is effective for removing copper from synthetic wastewater but not effective for nickel removal. For heavy metal/hydrogen binary systems, heavy metal-containing solutions can be concentrated by an ion-exchange/regeneration cycle. The experimental regeneration curve suggests that the separation factor α_{CuH} should be less than unity, i.e., selectivity reversal occurs in the regeneration cycle. Selected separation of copper and nickel is also feasible for the copper/nickel/hydrogen tertiary system. The conventional wave propagation theory using a constant resin capacity and constant separation factors gives simple yet satisfactory prediction of the breakthrough and regeneration curves of the ion-exchange process.

ACKNOWLEDGMENT

This work was supported by the National Science Council of Taiwan, Republic of China (Grant NSC84-2211-E-036-001).

REFERENCES

1. T. Vermeulen, D. LeVan, N. K. Hiester, and G. Klein, "Adsorption and Ion Exchange." In *Perry's Chemical Engineers' Handbook*, 6th ed. (R. H. Perry, D. W. Green, and J. O. Maloney, Eds.), McGraw-Hill, New York, NY, 1984.
2. R. A. Corbitt, *Standard Handbook of Environmental Engineering*, McGraw-Hill, New York, NY, 1990.
3. E. Maliou, M. Malamis, and P. O. Sakellarides, "Lead and Cadmium Removal by Ion-Exchange," *Water Sci. Technol.*, 25, 133 (1992).
4. B. W. Zhang, K. Fischer, D. Bieniek, and A. Kettrup, "Synthesis of Carboxyl Group Containing Hydrazine-Modified Polyacrylonitrile Fibers and Application for the Removal of Heavy-Metals," *Reactive Polym.*, 24, 49 (1994).
5. M. Ersöz, E. Pehlivan, H. J. Duncan, S. Yıldız, and M. Pehlivan, "Ion-Exchange Equilibria of Heavy-Metals in Aqueous-Solution on New Chelating Resins of Sporopollenin," *Ibid.*, 24, 195 (1995).



6. A. U. Baes, S. J. P. Umali, and R. L. Mercado, "Ion-Exchange and Adsorption of Some Heavy-Metals in a Modified Coconut Coir Cation-Exchanger," *Water Sci. Technol.*, **34**, 193 (1996).
7. C. N. Mazidji, B. Koopman, and G. Bitton, "Chelating Resin Versus Ion-Exchange Resin for Heavy-Metal Removal in Toxicity Fractionation," *Ibid.*, **26**, 189 (1992).
8. D. Petruzzeli, R. Passino, and G. Tiravanti, "Ion Exchange Process for Chromium Removal and Recovery from Tannery Wastes," *Ind. Eng. Chem. Res.*, **34**, 2612 (1995).
9. N. Sapari, A. Idris, and N. H. Abhamid, "Total Removal of Heavy-Metal from Mixed Plating Rinse Waste-Water," *Desalination*, **106**, 419 (1996).
10. D. A. Clifford, "Multicomponent Ion-Exchange Calculations for Selected Ion Separations," *Ind. Eng. Chem., Fundam.*, **21**, 141 (1982).
11. D. A. Clifford and R. E. Majano, "Computer Prediction of Ion Exchange," *J. Am. Water Works Assoc.*, **85**, 20 (1993).
12. D. A. Clifford and X. Liu, "Ion Exchange for Nitrate Removal," *Ibid.*, **85**, 135 (1993).
13. X. Liu and D. A. Clifford, "Ion-Exchange with Denitrified Brine Reuse," *Ibid.*, **88**, 88 (1996).
14. J.-M. Chern and S.-N. Huang, "Study of Nonlinear Wave Propagation Theory. 1. Dye Adsorption by Activated Carbon," *Ind. Eng. Chem. Res.*, **37**, 253 (1998).
15. J.-M. Chern and S.-N. Huang, "Study of Nonlinear Wave Propagation Theory. II. Interference Phenomena of Single-Component Dye Adsorption Waves," *Sep. Sci. Technol.*, **34**, 1993 (1999).
16. F. G. Helfferich and G. Klein, *Multicomponent Chromatography: Theory of Interference*, Dekker, New York, NY, 1970.
17. F. G. Helfferich, "Multicomponent Ion Exchange in Fixed Beds: Generalized Equilibrium Theory for Systems with Constant Separation Factors," *Ind. Eng. Chem., Fundam.*, **6**, 362 (1967).
18. F. G. Helfferich, "Conceptual View of Column Behavior in Multicomponent Adsorption or Ion Exchange Systems," *AIChE Symp. Ser.*, **80**, 1 (1984).
19. F. G. Helfferich and P. W. Carr, "Non-linear Waves in Chromatography: I. Waves, Shocks, and Shapes," *J. Chromatogr.*, **629**, 97 (1993).
20. F. G. Helfferich and R. D. Whitley, "Non-linear Waves in Chromatography: II. Wave Interference and Coherence in Multicomponent Systems," *J. Chromatogr. A*, **734**, 7 (1996).
21. F. G. Helfferich, "Non-linear Waves in Chromatography: III. Multicomponent Langmuir and Langmuir-like Systems," *Ibid.*, **768**, 169 (1997).
22. F. G. Helfferich, *Ion Exchange*, McGraw-Hill, New York, NY, 1962.

Received by editor July 29, 1998

Revision received March 1999



Request Permission or Order Reprints Instantly!

Interested in copying and sharing this article? In most cases, U.S. Copyright Law requires that you get permission from the article's rightsholder before using copyrighted content.

All information and materials found in this article, including but not limited to text, trademarks, patents, logos, graphics and images (the "Materials"), are the copyrighted works and other forms of intellectual property of Marcel Dekker, Inc., or its licensors. All rights not expressly granted are reserved.

Get permission to lawfully reproduce and distribute the Materials or order reprints quickly and painlessly. Simply click on the "Request Permission/Reprints Here" link below and follow the instructions. Visit the [U.S. Copyright Office](#) for information on Fair Use limitations of U.S. copyright law. Please refer to The Association of American Publishers' (AAP) website for guidelines on [Fair Use in the Classroom](#).

The Materials are for your personal use only and cannot be reformatted, reposted, resold or distributed by electronic means or otherwise without permission from Marcel Dekker, Inc. Marcel Dekker, Inc. grants you the limited right to display the Materials only on your personal computer or personal wireless device, and to copy and download single copies of such Materials provided that any copyright, trademark or other notice appearing on such Materials is also retained by, displayed, copied or downloaded as part of the Materials and is not removed or obscured, and provided you do not edit, modify, alter or enhance the Materials. Please refer to our [Website User Agreement](#) for more details.

Order now!

Reprints of this article can also be ordered at
<http://www.dekker.com/servlet/product/DOI/101081SS100100214>